OPTIMAL DESIGN OF STRETCHERS POSITIONS
OF MORTISE AND TENON JOINT CHAIR

Wen-Gang Hu, Wei-Lian Fu, Hui-Yuan Guan
Nanjing Forestry University
College of Furnishings and Industrial Design
Nanjing, China

ABSTRACT

The chair joined by oval mortise-and-tenon was taken as a case. Then influences of two adjacent sides (side A and side B) stretcher positions on mechanical properties of chairs, including ultimate loading capacity, stiffness and strain distributions, were investigated through using experimental and numerical methods. Firstly, two factors and three levels experiments were conducted and analyzed by Finite Element Method (FEM) . The results showed that ultimate loading capacity of chairs decreased firstly and then increased with the growth of the height of stretchers positions. In addition, the stress concentration occurred at middle of side rails and joints of side rails, especially at the side B, while the stress at the middle of the leg was minimum. Besides, the higher the stretcher position of the side A was, the more harmonious the stress distributions of chair was, and the higher ultimate loading capacity and stiffness were. Moreover, the results of FEM were well consistence with those of experiments, and the errors were within 10%. Secondly, two factors and five levels numerical analysis was conducted to optimize the stretcher positions of chair by the FEM, and the results showed more boadly that the best stretchers positions of chair owning the highest loading capacity was not the only one. Finally, the relationship between ultimate loading capacity and stretcher positions was generated by using the response surface method, and the correlation coefficient was nearly 88%.

KEYWORDS: Optimal design, chair, stretcher position, FEM, mortise-and-tenon.

INTRODUCTION

Furniture is one kind of wood products that consuming lots of high quality wood resources, especially the solid wood furniture. Most methods of trying to reduce the cost and increase the lumber recovery mainly paied attention on processing equipment and technology. It ignored the root of this problem was structure design of furniture. However, the design of furniture still remained at the stage where the design laid on experience or simple analysis simplifying furniture

as two-demension structure, but it was not able to reflect the real state of three-demensional structure, especially the solid wood mortise-and- tenon furniture.

Recently, most studies on mechanical properties of mortise-and-enon joint furniture mainly concentrated on factors influencing the strength of joint, including shaps of joint (Tankut et al. 2005), fit of joint (Dzincic and Skakic 2012), size of tenon (Kasal et al. 2016a), tree species and glue (Smardzewski et al. 2002; 2008, Ratnasingam 2013). Besides, T-shaped and L-shaped specimens were used to conduct experiments to get the best parameters (Derikvand and Smardzewski 2013, Kasal et al. 2015) which was used to instruct the optimal design of the mortise-and-tenon joint furniture. Admittedly, although the strength of component was enough to carry the load that furniture beared, it was the jont that determined the strength of the whole structure of furniture. In other words, the mechanical properties of mortise-and-tenon joint furniture depended on the strength of joint not components (Eckelman 1971, Smardzewski and Lewandowski 2014, Hu et al. 2017). However, sometimes it is not that the stronger the joint is, the more reasonable the furniture structure is. The positions of stretchers also play an important role. Unfortunately, few studies on mechanical properties of the entire furniture were conducted. Kasal et al. (2016 b) investigated the relationship between the individual joint strength and chair strength, and the equation between the front to back loading capacity of chair and the moment capacities of T-shaped and L shaped joints were derived in two-dimensional structure. Besides, Aydin and Ergün (2016) studied the chair frames with various stretcher positions by FEM in two-dimensional structure. The results showed that frames without stretchers yield more deformation, and use of stretcher reduced the stresses and deformations in the frames. In addition, the FEM provided comparable deformation values to the real behavior.

There is no doubt that the joint is the weakest part of the mortise-and-tenon joint furniture, but it is not necessary to pursue the highest strength and ignored the entire structure of furniture, which leads to increase the volume of wood and cost. Thus, the aim of this paper is to investigate the influences of stretchers positions on mechanical properties of mortise-and-tenon joint furniture taking chairs in three-dimensional structure joined by oval tenon as a case. The ultimate loading capacity, stiffness and the strain distributions of chairs were determined and the influences of stretchers positions on the entire strength of chairs were analyzed by conducting the experiments. Subsequently, the equation between the ultimate loading capacity of chairs and stretcher positions was derived by the response surface method. Besides, the stress distributions of chairs were analyzed by FEM, and the results of FEM were compared with those of experiment. Finally, the stretcher positions was optimized based on FEM and response surface method.

MATERIAL AND METHODS

Test materials

All specimens were made with beech (*Fagus orientalis* Lipsky), bought from local commercial supplier (Nanjing, China). The average density was 0.712 g·cm^{-3}, and the moisture content of beech was conditioned to and held at 12.03% before and during the experiment. The mortise-and-tenon joint was glued with polyvinyl acetate (PVAc) which was produced by Pattex in China, and the solid content was 52%. The amount of applied glue was controlled by the gravimetric method and it was determined that it was 182±25 g·m^{-2}. In addition, the temperature was controlled in 22°C, and the relative humidity was 48% during the entire process of experiment. All specimens were processed by WPC Computer Numerical Control (CNC) machine with accuracy of 0.01 mm (YUANLI, China), and a 100 KN universal testing machine AG-IC (SHIMADZU, Japan) was applied to carry out the experiment with a fixture designed by authors shown in Fig. 1.
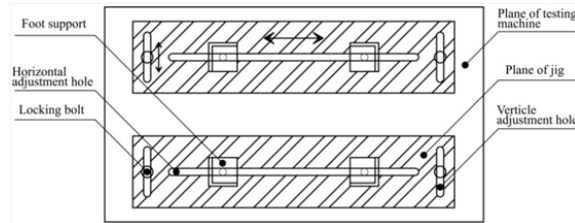
Fig. 1: The diagram of fixture.

It was made up of two steel planes of jig with four removable foot supports which were able to adjust to the size of chairs. Besides, static data acquisition instrument TDS-530 (TML, Japan) was applied to determine the strains distributions of the chair with strain gauges BFH120-3AA0D100.

Description of specimens

In general, the stretchers at two adjacent sides of chairs are staggered with each other to avoid the tenon conflict. This can increase the length of the tenon and get higher strength, when the cross section of leg is limited for solid wood mortise-and-tenon joint furniture design. Fig. 2 is the outline dimensions of chair used in experiments but the stretcher positions varied. Besides, the detail dimensions of mortise and tenon are shown in Fig. 3, the cross section of leg is shown in Fig. 3a, Fig. 3b is the size of mortise, and Fig. 3c is the length and width of tenon of stretcher and side rail, as well as the cross section of stretcher and side rail were shown in Fig. 3d and Fig. 3e respectively. In addition, the units of dimensions in figures are all millimeter (mm) without special emphasis. All specimens were stored for a week before conducting experiment.
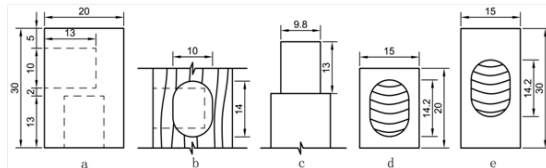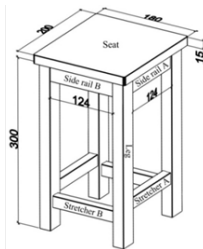

Fig. 2: The outline dimensions of chair.

Fig. 3: The dimensions of mortise and tenon.

Test methods

The stretcher positions of two adjacent sides are shown in Fig. 4, and the sides parallel to the wide direction of the leg and parallel to thick direction of legas were named as Side A and Side B respectively. Besides, the heights of stretcher A varied from 70 mm, 120 mm and 170 mm in Side A, and heights of stretcher B were 50 mm, 100 mm and 150 mm in Side B, which were named as A1, A2, A3 and B1, B2, B3 respectively. Thus, totally nine kinds of chairs were tested, and five times were repeated for each in 5000 N, 8000 N, 10000 N and 12000 N loading levels respectively. Then the stiffness of chairs were calculated by Eq. 1.
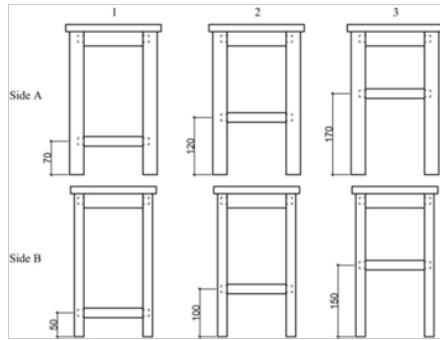
Fig. 4: The varied principle of stretcher .

$$K = F / U \tag{1}$$

where: K - entire stiffness of chair (N·mm⁻¹),
        F - loading level (N),
        U - displacement of center of seat (mm).

In addition, the strain distributions of chairs under four different loading levels were measured by static data acquisition instrument with quarter-bridge and three-line method. Since the chair used in the experiment is symmetric structure, so only one quarter of chair is pasted strain gauges, and the positions are at the middle of legs, stretchers and side rails, which is shown in Fig. 5a. Besides, positions 10 mm right below the stretcher joints and side rail joints are also pasted like Fig. 5b. Each position is pasted two perpendicular strain gauges, which are used to measure the horizontal strain and vertical strain respectively. The strain gauges with odd numbers are used to test the horizontal strain, while the even numbers are to measure the vertical strain. Fig. 5c is the experimental testing condition.
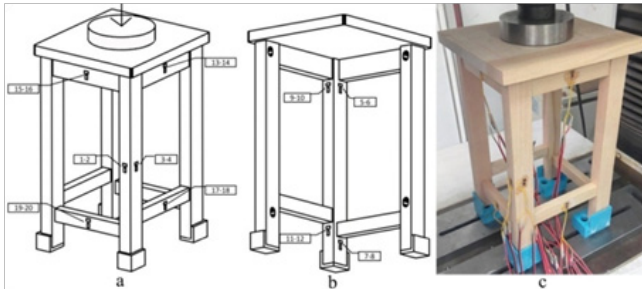

Fig. 5: The positions pasted strain gauges.

Method of establishing the FEM

Abaqus 6.14-1 was used to establish the FEM. The geometric size of the FEM was the same with the real dimensions of chair, and the mechanical properties of beech are shown in Tab. 1, which were measured by authors at the initial stage of this study (Hu and Guan 2017a), including the elastic constants, yield strength of beech, and strength of bonding interface in normal direction and two shear directions.

Tab. 1: Mechanical properties of materials used in joints.

Mechanical properties of wood (MPa)	Modulus of elasticity			Poisson ratio (dimensionless)						Tangential modulus		
	E_L	E_R	E_T	V_{LR}	V_{LT}	V_{RT}	V_{TR}	V_{TL}	V_{RL}	G_{LR}	G_{LT}	G_{RT}
	12205	1858	774	0.502	0.705	0.526	0.373	0.038	0.078	899	595	195
Yield strength (MPa)	Longitudinal			Radial						Tangential		
	42.51			9.83						4.49		
Interface strength (MPa)	Normal			Shear I						Shear I		
	1.63			3.78						3.48		

E_L, E_R, E_T: Modulus of elasticity in grain, radial, and tangential directions, respectively;

V_{LR}, V_{RT}, V_{LT}: Poisson ratio on grain-radial, radial-tangential, and grain-tangential planes, respectively;

G_{XY}, G_{YZ}, G_{XZ}: Kirchhoff modulus on grain-radial, radial-tangential, and grain-tangential planes, respectively. Shear I: The shear direction was parallel to the length of tenon. Shear I: The shear direction was vertical to the length of tenon.

Fig. 6 is the FEM of chair. The hexahedral shape element C3D8I was used to generate the mesh for beech, and the bonding interface was regarded as a new layer meshed with COH3D element.
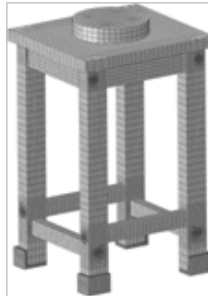

Fig. 6: The finite element model of chair.

Besides, foot supports and load head were meshed with discrete rigid element which was not deformable under loading condition. In addition, for curved surfaces of mortise and tenon, surface-to-surface contact was modeled, and the tangential behavior was friction with friction coefficient 0.54 (Hu and Guan 2017b, 2017c). By contrast, the flat surfaces of mortise-and-tenon joints were bonded by bonding interface (cohesive element). Then, the 3 mm displacement load and constraints were imposed on the FEM according to the experimental state of chairs. After analyzing, the stress distributions of the chair and the reaction force of loading head can be outputted, which can be used to compare with the experimental load values with the loading head at 3 mm displacement.

RESULTS AND DISCUSSION

Ultimate loading capacity and stiffness of chairs

Fig. 7 presents the relationship between the ultimate loading capacity and the height of stretcher A and stretcher B.
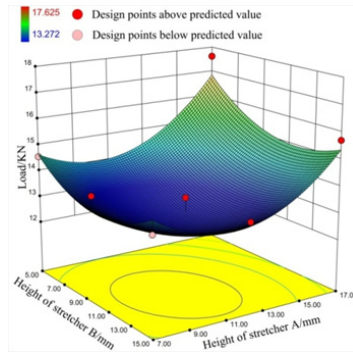
Fig. 7: Relationship between ultimate loading capacity and positions of stretcher A and B.

It indicated that the ultimate loading capacity of chair was decreased at the initial stage and increased at later stage with the growth of stretcher positions. The ultimate loading capacities were higher than others, when the position of stretcher A was at A3, wherever the positions of stretcher B were. However, the ultimate loading capacity was the minimum when the stretcher positions of both sides were at the middle of the leg. The equation between ultimate loading capacity and positions of stretcher A and stretcher B was figured out by the response surface method shown in Eq. 2, and the correlation coefficient was nearly 80%, which can satisfy the engineering request.

$$F = 23.26 - 0.77b - 12.20a - 0.01ab + 0.04b^2 + 0.06a^2 \qquad R^2 = 0.7924 \qquad (2)$$

where: F - ultimate loading capacity (N),
         a - height of stretcher A (mm),
         b - height of stretcher B (mm).

Fig. 8 shows the typical failure modes of nine kinds of chairs, which indicats that all chairs were damaged at the side rail B resulted from the fracture of the joint. It suggested that the joint of side rail B and leg was the weakest part of the chairs.
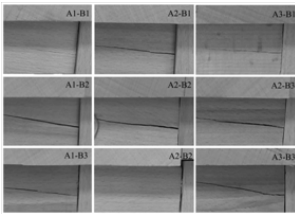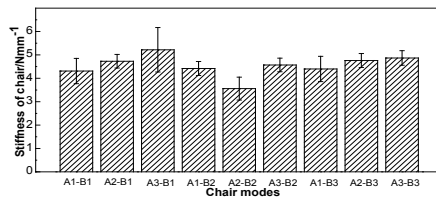

Fig. 8: The failure modes of chairs.

Fig. 9: The stiffness of chair.

The study on the stiffness of chairs under 12000 N loading level was investigated, which is presented in Fig. 9. The stiffness of the chairs are relativity higher than others when the position of stretcher A is at A3 and stretcher B is a certain constant. When the position of stretchers is A2-B2 (middle of the leg), the stiffness is the minimum. It indicats that the position of the stretcher A plays an significant role in the entire stiffness of chair, which had the same trendency

with the former study (Aydin and Ergün 2016). While the impact of stretcher B on stiffness of chair was not significant. Compared with the former studies (Hajdarević et al. 2015), the chair fram was regarded as two-dimensional structure, which was not able to reflect the real structure of chair.

Strain distributions of chairs

Fig. 10 shows the strain distributions of nine chair modes under different loading levels, and the positive values represent the tensile strains, while the negative values are compressing strains. On the whole, the strain magnitude of chairs increase with the growth of the loading levels. Besides, strain distributions are more harmonious than other chair modes, when the position of stretcher A is at A3, which suggests that the stretcher position is more reasonable than others. The reason is that with the increasing of position of stretcher A, it shares more load instead of side rail A, and then transferred to the entire frame to make chairs more stable. Together with ultimate loading capacity and stiffness of chairs, the position of stretcher A influences the mechanical properties of chairs significantly. In addition, former studies (Derikvand and Ebrahimi 2014, Aydin and Ergün 2016) investigated the strain distributions of 2D-dimensional chair frames by FEM.
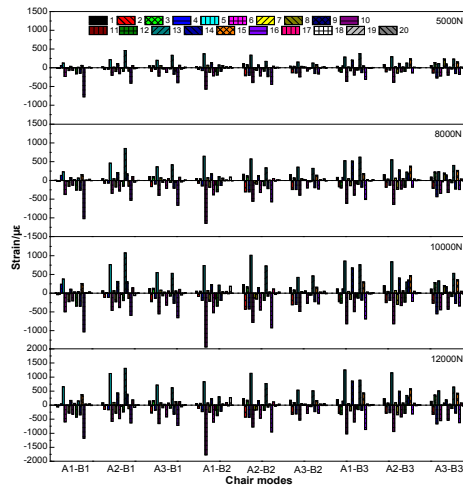

Fig. 10: Strain distribution of chairs.

Furthermore, the strains of every point pasted the strain gauges were compared, which can be found that the strains at the middle of side rail A (13-14), joint of said rail A (9-10) and that of side rail B (15-16,5-6) are higher than other points. It mean that it is easy to be stress concentration since bearing the main load transferred from the seat. Besides, the strains in joint of stretcher B (5-6) are higher than that of stretcher A (9-10). Together with the failure modes of chairs (Fig. 8), it also confirms that the joint of side rail B is the weakest part of the chair. In addition, the strains of following points 1-2, 3-4, 17-18 and 19-20 are relatively lower, which suggests that the stress at the middle of leg and stretcher are smaller than other points. Moreover, when the position of stretcher A is at A3, the strains at joint of side rail B (5-6) are lower than other chair modes, so it also indicates that the position of stretcher A influenced the strain distributions of chair significantly once again.

Results of FEM

The FEM of nine chairs were established and analyzed, and stress distributions of them were in the same trend. Taking the chair mode A1-B1 as an example, and the stress distribution of the chair in the process of loading are shown in Fig. 11. It suggests that the stress mainly concentrated on the middle and joint of side rails, as well as the foot supports, and the stress at the middle of legs and stretchers are relatively lower than other points. Besides, Fig. 12 shows the stress distributions of joint in side rail A and joint of side rail B, it is obvious that the stress concentration at joint of side rail B is more significant than that of side rail A.
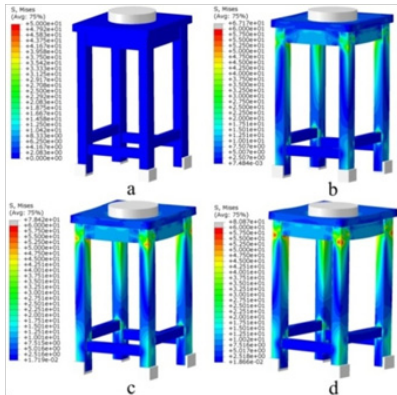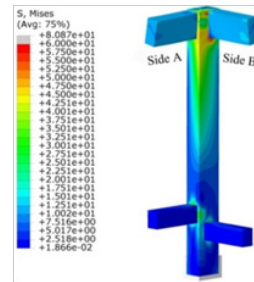

Fig. 11: Stress distributions of chair.

Fig. 12: Stress distributions of joint.

The loads outputted by test machine were compared with FEM with the displacement of loading head was 3 mm, which is shown in Fig. 13. It indicates that the results of the experiment are well consistence with those of the FEM, and the maximum load was determined when the chair mode is A3-B1. Besides, the errors between experiment and FEM of 9 chairs are all within 10%. The accuracy of FEM is higher than related studiy (Yorur et al. 2016). Based on the above analysis, it confirms that the FEM established in the article is suitable to apply to solid wood mortise and tenon furniture optimal design.
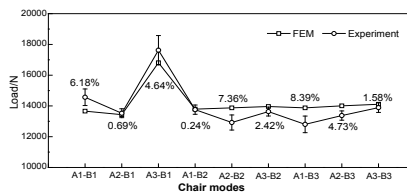

Fig. 13: Comparison between experiment and FEM.

Optimization of the stretcher positions

A two factors and three levels experiments were conducted and numerically analyzed by FEM with the maximum height of stretcher A and stretcher B only 170 mm and 150 mm respectively. However, the total length of leg is 270 mm (minus the width of side rail 30 mm), so a further study is necessary. Two additional levels are added to position of stretcher A and stretcher B named A4, A5 and B4, B5, and the height of them are 200 mm, 250 mm, 180 mm and 230 mm

respectively. Then a two factors and five levels experiment with totally 25 kinds of chairs are needed conducting. In order to save time and costs, the FEM is used to analyze the rest of tests.

Together with the above study, 25 kinds of chair modes were established based on FEM. Besides, 3 mm displacement was applied to the loading head, then the reaction forces of loading head were obtained. The results are shown in Fig. 14, which indicats that when the height of stretcher A is at A4, A5 and stretcher B is at B1, B2 and B3, as well as A3-B1, the reaction forces are bigger than other chair modes. In other words, it can be presented that the height of stretcher A was 2/3 greater than the length of leg, and that of stretcher B is 1/2 smaller than length of leg, or the stretcher A is 1/2 greater than length of leg, and the stretcher B is 1/6 smaller than length of leg.
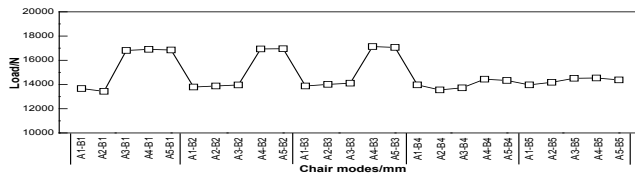

Fig. 14: The ultimate loading capacity of 25 kinds of chairs.

In order to make it more general, the response surface method was used to fit the relationship between ultimate loading capacity and heights of stretcher A and stretcher B, which is shown in Fig. 15, and Eq. 3.
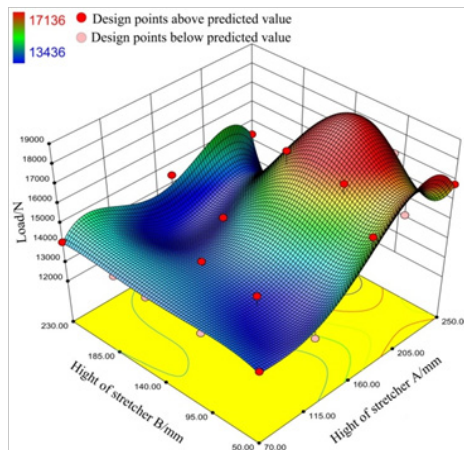

Fig. 15: Relationship between loading capacity of chairs and stretcher positions.

$$F = 19524 + 372a - 659b + 0.43ab - 4.8a^2 + 8.4b^2 - 4.6e^{-3}a^2b + 3.7e^{-4}ab^2 + 0.026a^3 - 4.4e^{-2}b^3 - 1.8e^{-5}a^2b^2 + 2.03e^{-5}a3b + 1.1e^{-5}ab^3 - 4.9e^{-5}a4 + 7.7e^{-5}b^4 \qquad R^2 = 0.88 \qquad (3)$$

where: F - ultimate loading capacity (N);
  a - height of stretcher A (mm);
  b - height of stretcher B (mm)

CONCLUSIONS

In conclusion, the influences of stretcher positions on mechanical properties of chairs were investigated by experimental and numerical methods, including ultimate loading capacity, stiffness and strain distributions of chairs. Finally, the stretcher positions were optimized based on FEM and response surface method, and the final conclusions were as followings:

1) With the growth of positions of stretcher A and stretcher B, the ultimate loading capacity showed a trend that decreased at first and then increased. Besides, ultimate loading capacity and stiffness were generally higher than others, when the position of stretcher A was at A3. However, when the position of stretchers was at A2-B2, the ultimate loading capacity and stiffness were all the minimum.

2) Through strain measuring, the strains at the middle of side rails (13-14, 15-16) and the joints of stretchers (5-6, 9-10) were higher than other parts. In addition, stress concentrated on the joint of side rail B (5-6) was more significant than others. While, the stress distributions at the middle of legs (1-2, 3-4) and middle of stretchers (17-18, 19-20) was relatively lower than other points. Besides, when the position of stretcher A was at A3, the strain distributions of chairs were more harmonious.

3) Together with ultimate loading capacity, stiffness and strain distributions of chairs, the results of FEM were well consistence with that of experiment, and the errors of 9 chair modes were all within 10%. It indicated that the FEM established in the article can be applied to optimal design of solid wood mortise-and-tenon joint furniture.

4) A general law which can be used in structure design of wood furniture and other wood products was obtained. Loading capacity was relatively higher when the height of stretcher A was 2/3 greater than length of leg, and that of stretcher B was 1/2 smaller than length of leg. Besides, the stretcher A was 1/2 greater than length of leg, and the stretcher B was 1/6 smaller than length of leg. In addition, the relationship between ultimate loading capacity and stretcher positions was generated on the bias of response surface method with correlation coefficient nearly 88%.

In conclusion, it is recommended to increase the dimension of side rails and the joints of them, and heighten the position of stretcher A in order to decrease the stress concentration and make the design more reasonable. Besides, the cost can be cut by reducing the volume of wood at middle of legs and stretchers. Furthermore, the methods studied in this article are also suitable for other wood productions and wooden constructure.

ACKNOWLEDGMENTS

REFERENCES

1. Aydin, T.Y., Ergün, G., 2016: Finite element (FE) analysis of chair frames constructed with Turkish red pine *Pinus brutia* ten.).1st International Mediterranean Science and Engineering Congress (IMSEC 2016) 26-28 October, Adana, TURKEY, Pp 2043-2049.
2. Dzincic, I., Skakic, D., 2012: Influence of type of fit on strength and deformation of oval tenon-mortise joint, Wood Research 57 (3): 469-477.

3. Derikvand, M., Ebrahimi, G., 2014: Finite element analysis of stress and strain distributions in mortise and loose tenon furniture joints, Journal of Forestry Research 25(3): 677–681.

4. Derikvand, M., Smardzewski, J. 2013: Withdrawal force capacity of mortise and loose tenon T-type furniture joints, Turk J Agric For 37: 469-478.

5. Eckelman, C.A., 1971: Bending strength and moment rotation characteristics of two-pin moment resisting dowel joints, Forest Prod J 21(3): 35-39.

6. Hajdarević, S., Busuladžić, I., 2015: Stiffness analysis of wood chair frame, Procedia Engineering 100: 746-755.

7. Hu, W.G., Bai, J., Guan, H.Y. 2017: Investigation on a method of increasing mortise and tenon joint strength of fast growing wood, Journal of Beijing Forestry University 39(4): 101-107.

8. Hu W.G., Guan, H.Y., 2017a: Study on elastic modulus of beech in different stress states, Journal of Forestry Engineering 2(6): 31-36.

9. Hu, W.G., Guan, H.Y., 2017b: Investigation on withdrawal force of mortise and tenon joint based on friction properties, Journal of Forestry Engineering 04: 158-162.

10. Hu, W.G., Guan, H.Y. 2017c: Experimental and numerical study on optimization design of stretcher positions, Wood research 62(4): 575-586.

11. Kasal, A., Eckelman, C. A., Haviarova, E., Yalcin, i., 2015: Bending moment capacities of L-shaped mortise and tenon joints under compression and tension loadings, BioResources 10(4): 7009-7020.

12. Kasal, A., Kuskun, T., Haviarova, E., Erdil, Y.Z., 2016a: Static front to back loading capacity of wood chairs and relationship between chair strength and individual joint strength, BioResources 11(4): 9359-9372.

13. Kasal, A., Smardzewski, J., Kuşkun, T., Erdil, Y. Z., 2016b: Numerical analyses of various sizes of mortise and tenon furniture joints, BioResources 11(3):6836-6853.

14. Kayjin, B., Yorur, H., Uysal, B., 2016: Simulating strength behaviors of corner joints of wood constructions by using finite element method, Drvna Industrija 67(2): 133-140.

15. Ratnasingam, J., Iorasn, F., 2013: Effect of adhesive type and glue-line thickness on the fatigue strength of mortise and tenon furniture joints, Eur. J. Wood. Wood. Prod. 71(1): 819-821.

16. Smardzewski, J., 2002: Strength of profile-adhesive joints, Wood Science and Technology 36 (2): 173-183.

17. Smardzewski, J., 2008: Effect of wood species and glue type on contact stresses in a mortise and tenon joint, J. Mech. Eng. 222(12):2293-2299.

18. Smardzewski, J., Lewandowski, W., 2014: Elasticity modulus of cabinet furniture joints, Mater design 60(8): 260-266.

19. Tankut, A.N., Tankut, N., 2005: The Effects of Joint forms (Shape) and dimensions on the strengths of mortise and tenon joints. Turk. J. Agric. For. 29: 493-498.

Wen-Gang Hu, Wei-Lian Fu, Hui-Yuan Guan*
Nanjing Forestry University
College of Furnishings and Industrial Design
210037 Nanjing
China
Phone: 150-7787-2795
*Corresponding author: hwg@njfu.edu.cn